

Modeling Label Semantics Improves Activity Recognition

Xiyuan Zhang, Ranak Roy Chowdhury, Dezhi Hong[†], Rajesh K. Gupta, Jingbo Shang
 University of California, San Diego, La Jolla, CA, USA, [†]Amazon
 xiuyanzh@ucsd.edu, {rrchowdh, gupta, jshang}@eng.ucsd.edu, hondezhi@amazon.com

ABSTRACT

Human activity recognition (HAR) aims to classify sensory time series into different activities, with wide applications in activity tracking, healthcare, human computer interaction, etc. Existing HAR works improve recognition performance by designing more complicated feature extraction methods, but they neglect the label semantics by simply treating labels as integer IDs. We find that many activities in the current HAR datasets have shared label names, e.g., “open door” and “open fridge”, “walk upstairs” and “walk downstairs”. Through some exploratory analysis, we find that such shared structure in activity names also maps to similarity in the input features. To this end, we design a sequence-to-sequence framework to decode the label name semantics rather than classifying labels as integer IDs. Our proposed method decomposes learning activities into learning shared tokens (“open”, “walk”), which is easier than learning the joint distribution (“open fridge”, “walk upstairs”) and helps transfer learning to activities with insufficient data samples. For datasets originally without shared tokens in label names, we also offer an automated method, using OpenAI’s ChatGPT, to generate shared actions and objects. Extensive experiments on seven HAR benchmark datasets demonstrate the state-of-the-art performance of our method. We also show better performance in the long-tail activity distribution settings and few-shot settings.

KEYWORDS

Human Activity Recognition; Label Name Semantics; Time series; Augmentation

1 INTRODUCTION

Sensor-based human activity recognition (HAR) identifies human activities using readings from wearable devices. HAR has a variety of applications including healthcare, motion tracking, smart home automation, human computer interaction [6, 9, 19, 26, 31, 53]. For example, acceleration sensors attached to legs record subjects walking around and performing daily activities for gait analysis for Parkinson’s disease patients [2]; accelerometer and gyroscope can monitor user postures to detect falls for elderly people [48]. While tremendously valuable, human activity data remain difficult to collect due to security or privacy concerns.

We note that existing HAR methods treat labels simply as integer class IDs and learn their semantics purely from annotated data. This is less effective especially when labeled data are limited. To achieve better recognition performance, the line of research relies mostly on designing better handcrafted statistical features [3, 15] or automated feature extraction through deep models like CNN, RNN, Transformer and their combinations [21, 25, 27, 53, 54, 58]. These methods in the literature neglect the potential benefits of modeling label name semantics. We argue that a better way to

learn activity semantics is through label name modeling, as activity names often share sub-structure in HAR datasets. Figure 1a illustrates an example set of label names in typical HAR datasets. Different activities have common words in their label names. For example, “eat pasta” and “each sandwich” both have “eat” as prefix for describing the action; “open drawer” and “close drawer” both act on the object “drawer”. Such shared label structure indicates the similarity embedded in the original sensory activity data. As shown in Figure 1b, we apply T-SNE visualization on sensory readings from the Opportunity dataset [39]. We color different activities by common actions or common objects. Activities of the same color (sharing the same action or object in label names) appear closer in the embedding space, indicating stronger similarity in the original sensory measurements. Since activities sharing label names also have similar patterns in the input features, this motivates us to find a more efficient learning framework that promotes knowledge transfer of shared tokens across different activities.

To this end, we propose a semantic HAR model, SemanticHAR, shown in Figure 2, which models both input sensory data features and label name semantics. SemanticHAR comprises an encoder for extracting features from sensory input, and a decoder for predicting label names. Unlike existing HAR models that output integer class IDs as prediction results, SemanticHAR outputs label name sequences, thus preserving relationships among various activities. During training, we optimize the model by minimizing the difference between predicted label names and ground-truth label names. During inference, we exploit a constraint decoding method to ensure that all the generated labels are valid. We further introduce a label augmentation strategy that randomly replaces the original label sequences by their meaningful tokens (e.g., all actions of “open X” are treated as a class of “open”). This helps the model better capture semantics of shared tokens across different activities. For HAR datasets that originally do not have shared sub-structure, we also offer an automated label generation method to generate new labels with shared tokens and same semantic meanings, leveraging OpenAI’s large language chatbot ChatGPT. To the best of our knowledge, this is the first HAR model that performs a classification task based on decoding label structure. We evaluate SemanticHAR on HAR benchmark datasets and observe state-of-the-art performance.

We summarize our main contributions as follows:

- We find shared structure in label names maps to similarity in the input data, leading to a more efficient new framework SemanticHAR based on modeling label name semantics. SemanticHAR decomposes learning activities into learning separate tokens and promotes knowledge transfer of shared tokens across activities.
- We propose label augmentation to consolidate semantics of shared tokens across different activities. We also leverage ChatGPT for an automated label generation approach for datasets originally without shared tokens.

[†]Work unrelated to Amazon.

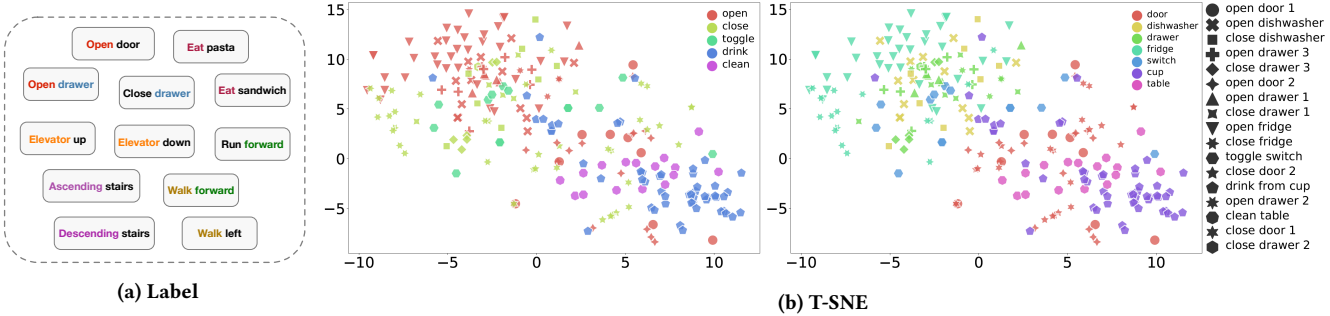


Figure 1: (a) Labels in HAR datasets typically share common words. (b) T-SNE visualization of sensory data in Opportunity dataset [39]. Each point represents one data sample, and each marker represents one type of activity. The two figures have the same set of data points and markers, and only differ in colors. The same color represents common actions (left figure) or common objects (right figure). Activities with the same actions or objects (marked by the same colors) are closer.

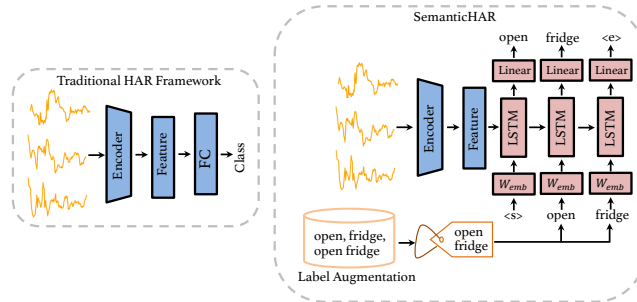


Figure 2: Comparison of existing HAR training framework and our sequence-to-sequence SemanticHAR. SemanticHAR generates label name sequence rather than simply treating labels as integer IDs. During training of SemanticHAR, we apply label augmentation and teacher forcing based on augmented labels. W_{emb} , $\langle s \rangle$, $\langle e \rangle$ represent linear embedding layer, start token, and end token.

- We evaluate SemanticHAR on seven HAR benchmark datasets and observe the new state-of-the-art performance. We also experiment under few-shot settings and observe even greater improvement.

Reproducibility. We will release the code at GitHub.

2 RELATED WORK

2.1 Human Activity Recognition

Existing HAR approaches can be categorized into statistical methods and deep learning based methods [7, 57]. Traditional machine learning methods are based on data dimensionality reduction, spectral feature transformation (e.g., Fourier transformation), kernel embeddings [35] or handcrafted statistical feature extraction (e.g., mean, variance, maximum, minimum) [15]. In recent years, deep learning advances automatic feature extraction and begins to substitute hand-crafted feature engineering in HAR [14, 17]. Various deep learning architectures have been explored, including convolutional neural network [21, 37, 52], recurrent neural network [16],

attention mechanism [25, 30] and their combinations [33, 53]. We shall note that these models focus on designing more effective feature extractors for better performance but neglect the semantic information in label names, which is the focus of this work.

2.2 Time-Series Classification

HAR data are time-stamped sensory series, enabling the use of time-series classification methods. Existing time-series classification models fall into two categories: statistical methods and deep learning based methods. Statistical methods are based on nearest neighbor [3, 42], dictionary classifier [40], ensemble classifier [28, 41], etc. Deep learning methods are based on convolutional networks [12, 13, 20, 27, 43, 46, 51], recurrent neural networks [22, 23], attention network [10, 54, 58], graph neural network [55]. Similar to existing HAR methods, time-series classification models focus on designing more advanced feature extraction or representation methods without taking into account the label semantics, whereas SemanticHAR models the shared sub-structure in the label set for more effective representation learning.

2.3 Label Semantics Modeling

Given label name semantics as prior knowledge, classification tasks could benefit from modeling such semantics through knowledge graph [45] or textual information [24, 36, 59]. Tong et al. [44] exploit knowledge from video action recognition models to construct an informative semantic space that relate seen and unseen activity classes. Recent works for zero-shot learning in human activity recognition also combine semantic embeddings [32, 50]. Unlike these works, SemanticHAR is a sequence-to-sequence HAR framework that decomposes learning activities and enables knowledge sharing through decoding label names.

3 PROBLEM SETTING

We focus on human activity recognition such as walking and sitting, using the sensory time-series data in a given time period. We denote the time-series input as $\mathbf{X} \in \mathbb{R}^{T \times c}$, where T is the length of each sequence, and c is the number of measured variables. We denote the corresponding human activity label set as $\mathbf{Y} = \{y_1, y_2, \dots, y_n\}$, where n is the size of the label set \mathbf{Y} . Each label y_i in the label set

Algorithm 1 SemanticHAR Pipeline

Input: Training set containing sensory sequence and label set, $D_{tr} = \{X_{tr}, Y_{tr}\}$, test set containing sensory sequence and label set $D_{te} = \{X_{te}, Y_{te}\}$

Model Parameter: Encoder θ , Decoder ϕ

Output: Predicted label sequence \hat{Y}_{te}

```

1: while not converged do
2:   Label augmentation on  $Y_{tr}$  to obtain  $Y'_{tr}$ 
3:   Encoder  $\theta$  extracts feature vector  $f$  from  $X_{tr}$ 
4:   Decoder  $\phi$  predicts label sequence  $P_\phi(\hat{Y}_{tr}|f)$ 
5:   Optimize  $\theta$  and  $\phi$  through  $\mathcal{L} = -\sum_{y \in Y'_{tr}, \hat{y} \in \hat{Y}_{tr}} y \cdot \log(\hat{y})$ 
6: end while
7: Encoder  $\theta$  extracts feature vector  $f$  from  $X_{te}$ 
8: Decoder  $\phi$  predicts label sequence  $P_\phi(\hat{Y}_{te}|f)$ 
9: return  $\hat{Y}_{te}$ 

```

Y is composed of a word sequence $y_i = [y_{i1}, y_{i2}, \dots, y_{ik_i}]$, where k_i is the length of the word sequence for the i -th label y_i . For example, label “walk upstairs” contains a word sequence of length two, [“walk”, “upstairs”] respectively. In label set Y , there exists shared structure across different labels. For example, “walk upstairs” and “walk downstairs” both have “walk” in label names. Formally, there exist labels $y_i, y_j, i \neq j$ that have the same word $y_{im} = y_{jl}$, where $1 \leq m \leq k_i, 1 \leq l \leq k_j$ are positions in y_i and y_j .

4 METHODOLOGY

We design a sequence-to-sequence architecture, SemanticHAR, to exploit label semantics embedded in the shared label structure for more efficient learning across activities, compared with existing HAR methods that simply treat labels as integer IDs (Figure 2). The input are segmented sensory readings measuring multiple variables. We first pass the input to an encoder for feature extraction and obtain a feature vector. The feature vector is used for initialization in the decoder. We adopt Long Short-Term Memory (LSTM) [18] as the decoder, so feature vector is used for initializing hidden state and cell state of LSTM. During inference, to guarantee all generated labels are valid, we adopt a constraint decoding method (Figure 3). We start from the start token and iterate over all the possible label names in the label set. We calculate the probability of decoding each label name sequence and choose the sequence with the highest probability as the final predicted label. During training we decode until reaching the ground truth sequence length and pad the remaining; during inference we decode until predicting the end token. We optimize SemanticHAR based on cross entropy loss between the predicted label name sequence \hat{y} and the ground truth label name sequence y :

$$\mathcal{L} = - \sum_{t=1}^k y_t \cdot \log(\hat{y}_t), \quad (1)$$

where k is the label sequence length. We summarize the overall training algorithm in Algorithm 1.

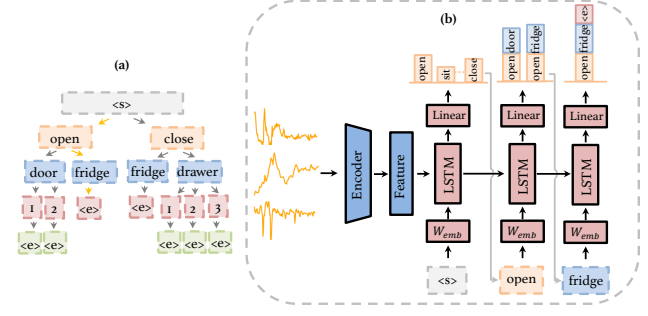


Figure 3: SemanticHAR inference process. (a) presents all possible paths. (b) shows the decoding process for one example path (“ s ” open fridge e ”), path marked by yellow). We inference each path in (a) and path with the overall highest score is the prediction for the input series. For one specific path, each decoding step takes the partially decoded path from the previous step as input and each path ends until we decode the end token e . Bars on the top represent scores for the partially decoded path up to the current step.

4.1 Encoding Features

Convolutional Neural Network (CNN) demonstrates advanced performance in various tasks like image recognition, object detection, and time-series classification [11, 46]. We apply one-dimensional convolutional neural network as encoder to extract features in human activity sensory readings. Let X represent the input for a particular convolutional layer, to calculate the output we have:

$$Conv(X_t) = \sum_{i=-k}^k W_{k+i} \cdot X_{t+i}, \quad (2)$$

where W represents convolution filter weights, and $k = \frac{k_t-1}{2}$ with k_t representing kernel size along time dimension. For simplicity we omit the bias term in the formula. The basic block of our encoder is composed of a convolutional layer followed by a Batch Normalization (BN) layer and a ReLU activation layer:

$$Block(X) = ReLU(BN(X)). \quad (3)$$

Batch normalization layer helps improve the convergence speed and stability of the neural network. We stack multiple blocks for feature extraction and transform the result through a linear layer to obtain a feature vector f :

$$f = W_O \cdot O + b_O, \quad (4)$$

where W_O, b_O represent weight and bias for the linear transformation layer, and O denotes output from the last basic block. The extracted feature vector f will then be used for initializing hidden state and cell state in the LSTM decoder.

4.2 Decoding Label Names

Long Short-Term Memory (LSTM) is popular for modeling long range dependencies, and we apply LSTM for decoding label names. Following our notation in Problem Setting, we use $y = [y_1, y_2, \dots, y_k]$

to represent the label sequence and \mathbf{X} to represent the input sensory data. We further require that each label name sequence start from a start token $\langle s \rangle$ and end at an ending token $\langle e \rangle$. Specifically, $\mathbf{y} = [y_0, y_1, y_2, \dots, y_k, y_{k+1}]$, where $y_0 = \langle s \rangle$, $y_{k+1} = \langle e \rangle$. Decoding the token $\langle e \rangle$ means that we reach the end of the sequence. LSTM (parameterized by ϕ) estimates the conditional probability $P_\phi(y_1, y_2, \dots, y_{k+1} | \mathbf{X})$ of decoding label \mathbf{y} from \mathbf{X} , given the extracted features \mathbf{f} from the encoder:

$$P_\phi(y_1, y_2, \dots, y_{k+1} | \mathbf{X}) = \prod_{t=1}^{k+1} P_\phi(y_t | \mathbf{f}, y_0, y_1, \dots, y_{t-1}), \quad (5)$$

where $P_\phi(y_t | \mathbf{f}, y_1, y_2, \dots, y_{t-1})$ is computed as a softmax over all the words in the label set vocabulary.

More specifically, we first transform the extracted feature vector \mathbf{f} through two separate linear layers to initialize the hidden state \mathbf{h}_0 and cell state \mathbf{c}_0 of LSTM:

$$\mathbf{h}_0 = \mathbf{W}_{\mathbf{h}_0} \cdot \mathbf{f} + \mathbf{b}_{\mathbf{h}_0}, \quad (6)$$

$$\mathbf{c}_0 = \mathbf{W}_{\mathbf{c}_0} \cdot \mathbf{f} + \mathbf{b}_{\mathbf{c}_0}, \quad (7)$$

where $\mathbf{W}_{\mathbf{h}_0}, \mathbf{W}_{\mathbf{c}_0}$ denote weights of the linear layer, and $\mathbf{b}_{\mathbf{h}_0}, \mathbf{b}_{\mathbf{c}_0}$ denote biases of the linear layer.

For every decoding step t , each token in the label sequence $y_t \in \mathbf{y}$ is first fed into a linear embedding layer to obtain representation \mathbf{z}_t in the embedding space

$$\mathbf{z}_t = \mathbf{W}_{\text{emb}} \cdot y_t + \mathbf{b}_{\text{emb}}, \quad (8)$$

where $\mathbf{W}_{\text{emb}}, \mathbf{b}_{\text{emb}}$ denote weight and bias of the embedding layer. Then we apply LSTM to the embedded representation

$$\mathbf{i}_t = \sigma(\mathbf{W}_{ii}\mathbf{z}_t + \mathbf{b}_{ii} + \mathbf{W}_{hi}\mathbf{h}_{t-1} + \mathbf{b}_{hi}), \quad (9)$$

$$\mathbf{f}_t = \sigma(\mathbf{W}_{if}\mathbf{z}_t + \mathbf{b}_{if} + \mathbf{W}_{hf}\mathbf{h}_{t-1} + \mathbf{b}_{hf}), \quad (10)$$

$$\mathbf{g}_t = \tanh(\mathbf{W}_{ig}\mathbf{z}_t + \mathbf{b}_{ig} + \mathbf{W}_{hg}\mathbf{h}_{t-1} + \mathbf{b}_{hg}), \quad (11)$$

$$\mathbf{o}_t = \sigma(\mathbf{W}_{io}\mathbf{z}_t + \mathbf{b}_{io} + \mathbf{W}_{ho}\mathbf{h}_{t-1} + \mathbf{b}_{ho}), \quad (12)$$

$$\mathbf{c}_t = \mathbf{f}_t \odot \mathbf{c}_{t-1} + \mathbf{i}_t \odot \mathbf{g}_t, \quad (13)$$

$$\mathbf{h}_t = \mathbf{o}_t \odot \tanh(\mathbf{c}_t), \quad (14)$$

where $\mathbf{h}_t, \mathbf{c}_t$ denote hidden state and cell state at time t , $\mathbf{i}_t, \mathbf{f}_t, \mathbf{g}_t, \mathbf{o}_t$ are the input gate, forget gate, cell gate, output gate in LSTM, and \odot is the Hadamard product. At each decoding step t , we apply a linear layer on the hidden state \mathbf{h}_t to predict a distribution over all the possible words in the label set:

$$\hat{y}_t = \mathbf{W}_y \cdot \mathbf{h}_t + \mathbf{b}_y, \quad (15)$$

where $\mathbf{W}_y, \mathbf{b}_y$ denote the weight and bias of the linear prediction layer. During training, we adopt teacher forcing [49] where the ground truth label token y_t is used as input to be conditioned on for predictions of later tokens, as shown in Figure 2. The teacher forcing improves convergence speed and stability during training. During inference decoding, predicted label token \hat{y}_t from the current decoding step is used as input to be conditioned on for predicting future tokens, as shown in Figure 3.

In typical natural language processing tasks, e.g., machine translation, it is common to decode the sequence using beam search during inference. Beam search reduces the memory requirement

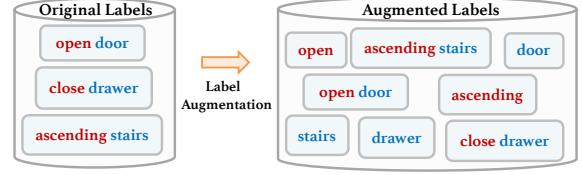


Figure 4: Illustration of our label augmentation strategy. We augment the original label name sequence by randomly choosing its meaningful tokens or the sequence itself.

by only tracking a pre-defined number of best partial solutions as candidates in decoding. In our label name decoding case, the size of the label set is relatively small, so we apply a *constraint decoding* method to calculate probability for all the valid sequences in the label set. We define valid partial sequence as the prefix sequence of the actual labels. Take “drink from up” as an example, valid partial sequences in this case include “drink”, “drink from” and “drink from up”. Formally, for a label $y_{1:k} = [y_1, y_2, \dots, y_k]$, valid partial sequences include all the prefixes $y_{1:t}, t \leq k$. The decoding is constrained in the sense that we only keep track of the valid partial sequences during decoding, and therefore the memory consumption is constant (the size of the label set). As shown in Figure 3, at step t , we calculate probability for all the valid partial sequences of length t , and pass them into the decoder for generating tokens at step $t+1$. The final inference prediction is the sequence that maximizes the overall sequence probability:

$$\hat{y} = \arg \max_{y \in Y} P_\phi(y | \mathbf{X}), \quad (16)$$

where X is the input test data, and Y is the label set.

4.3 Label Augmentation

To better learn the semantics of each word in the label sequence, we apply a label augmentation strategy as illustrated in Figure 4. During training, with some pre-defined probability we randomly choose meaningful single words from the original label sequence as the new labels. For example, an original label sequence “open drawer” contains single words “open” and “drawer”, so we randomly select from “open”, “drawer”, and “open drawer” as the new label during training. Following notation in Problem Setting, the original label $y_i = [y_{i1}, y_{i2}, \dots, y_{ik_i}]$, after label augmentation, we have a set of new labels $\{y_{i1}, y_{i2}, \dots, y_{ik_i}, y_i\}$, and for each iteration we randomly select one meaningful token from the new set of labels as the actual label. Note that since the goal of label augmentation is to help the model better capture semantics of different activities, we only choose meaningful single tokens in the original label sequences (e.g., actions and objects) as new labels. Other single tokens like stop words or numbers (e.g., “1” in “open door 1”) will not count as new labels. Also note that label augmentation is only applied during training, and during evaluation, the ground truth label stays the same as the original label. Because we adopt a constraint decoding method during inference, it is guaranteed that all the generated label sequences are valid sequences in the original label sets.

Table 1: Dataset statistics and example shared label names.

Dataset	Train	Test	Length	Channel	Class Num	Example Shared Label Names
Opportunity	2891	235	150	45	17	open door, open drawer, close drawer, open fridge, open dishwasher
PAMAP2	14438	2380	512	27	12	ascending stairs, descending stairs, walking, nordic walking
UCI-HAR	7352	2947	128	9	6	walk, walk upstairs, walk downstairs
USCHAD	17576	9769	100	6	12	run forward, walk forward, elevator up, elevator down, jump up
WISDM	12406	3045	200	6	18	eating soup, eating pasta, kicking soccer ball, playing tennis ball
Harth	14166	3588	300	6	12	sitting, standing, cycling sitting, cycling standing, cycling inactive

Table 2: Accuracy and Macro-F1 for SemanticHAR and baselines. We bold the best score and underline the second best.

Datasets	Metrics	DeepConvLSTM	XGBoost	MA-CNN	HHAR-net	THAT	Rocket	TST	SemanticHAR
Opp	Accuracy	0.746±0.049	0.688±0.017	0.549±0.029	0.753±0.027	0.803±0.012	0.811±0.008	0.784±0.018	0.847±0.015
	Macro-F1	0.634±0.036	0.547±0.011	0.416±0.036	0.620±0.021	<u>0.691±0.015</u>	0.670±0.016	0.668±0.023	0.741±0.029
PAMAP2	Accuracy	0.891±0.012	0.939±0.003	0.926±0.011	0.885±0.031	<u>0.943±0.005</u>	0.928±0.008	0.922±0.037	0.956±0.007
	Macro-F1	0.884±0.018	0.939±0.007	0.925±0.012	0.893±0.031	<u>0.949±0.005</u>	0.934±0.008	0.925±0.039	0.964±0.007
UCI-HAR	Accuracy	0.900±0.016	0.907±0.003	0.921±0.025	0.926±0.005	0.891±0.028	<u>0.939±0.002</u>	0.926±0.005	0.958±0.003
	Macro-F1	0.899±0.016	0.906±0.003	0.921±0.024	0.926±0.005	0.894±0.025	<u>0.942±0.002</u>	0.925±0.006	0.958±0.003
USCHAD	Accuracy	0.574±0.016	0.571±0.007	0.543±0.044	0.524±0.011	0.643±0.015	0.580±0.005	0.641±0.028	0.663±0.011
	Macro-F1	0.557±0.015	0.573±0.006	0.520±0.047	0.523±0.009	<u>0.619±0.012</u>	0.601±0.007	0.594±0.023	0.623±0.009
WISDM	Accuracy	0.689±0.014	0.668±0.005	0.634±0.059	0.566±0.016	0.643±0.007	<u>0.774±0.005</u>	0.715±0.003	0.793±0.007
	Macro-F1	0.685±0.013	0.662±0.006	0.631±0.060	0.538±0.012	0.634±0.005	<u>0.767±0.004</u>	0.710±0.004	0.786±0.008
Harth	Accuracy	0.979±0.006	0.977±0.001	0.973±0.016	<u>0.981±0.001</u>	0.960±0.016	0.897±0.003	0.974±0.005	0.982±0.003
	Macro-F1	<u>0.578±0.032</u>	0.522±0.003	0.538±0.025	0.515±0.049	0.485±0.025	0.472±0.019	0.501±0.031	0.583±0.020

5 EVALUATION

5.1 Datasets

We evaluate SemanticHAR and baselines on benchmark HAR datasets, summarized in Table 1. We split the data and define the window size generally based on previous works [10, 21].

Opportunity [39] is publicly available from the UCI Machine Learning Repository¹. The dataset collects readings from 4 users with 6 runs per user when users were performing daily activities. Sensors include body-worn sensors (IMU, 3D acceleration sensors, 3D localization information), object sensors (objects with 3D acceleration and 2D rate of turn), and ambient sensors (switches and 3D acceleration sensors). The full dataset includes annotations on multiple levels, and in this paper we use mid-level gesture annotations which contain shared label structure. Corresponding activities include opening door, closing fridge, drinking from cup, etc.

PAMAP2 [38] is publicly available from the UCI Machine Learning Repository². The dataset comprises readings collected from 9 subjects performing different physical activities (such as sitting, ascending stairs, etc.). Subjects wear 3 Inertial Measurement Units (IMU) at a sampling rate of 100 Hz as well as a heart rate monitor at a sampling rate of 9Hz during data collection. Three IMUs are positioned over the wrist on the dominant arm, on the chest and on the dominant side’s ankle, respectively.

UCI-HAR [1] is publicly available from the UCI Machine Learning Repository³. The dataset is collected from a group of 30 volunteers performing six different activities (walking, walking upstairs, walking downstairs, sitting, standing, and laying) with a Samsung

Galaxy S II smartphone on the waist. 3-axial linear acceleration and angular velocity were captured through embedded accelerometer and gyroscope at a sampling rate of 50Hz, and were then sampled in sliding windows. A set of feature vectors were further extracted from each sliding window in the time and frequency domain.

USCHAD [56] is publicly available at their data collection website⁴. 14 subjects participate in the data collection process by performing 12 low-level activities like walking forward, running forward, walking left. They use an off-the-shelf sensing platform MotionNode (6-DOF IMU designed for human motion sensing applications) to collect the datasets. To complete the study, each subject was asked to engage in each activity 5 times at different locations, both indoors and outdoors, over the course of multiple days.

WISDM [47] is publicly available from the UCI Machine Learning⁵. The dataset is collected from accelerometer and gyroscope sensors in smartphone and smartwatch at a rate of 20Hz. 51 subjects perform 18 activities for 3 minutes respectively.

Harth [29] is publicly available on Github⁶. 22 subjects participated in the collection process with recordings for 90 to 120 min during their regular working hours. They use two three-axial accelerometers attached to the thigh and lower back, and a chest-mounted camera (for data annotation) to collect data of 12 activities.

6 BASELINES AND METRICS

We compare SemanticHAR with a list of human activity recognition and time-series classification baselines, including both statistical approaches and state-of-the-art deep learning based models:

¹<https://archive.ics.uci.edu/ml/datasets/opportunity+activity+recognition>

²<https://archive.ics.uci.edu/ml/datasets/pamap2+physical+activity+monitoring>

³<https://archive.ics.uci.edu/ml/datasets/Human+Activity+Recognition+Using+Smartphones>

⁴<https://sipi.usc.edu/had/>

⁵<https://archive.ics.uci.edu/ml/datasets/WISDM+Smartphone+and+Smartwatch+Activity+and+Biometrics+Dataset+>

⁶<https://github.com/ntnu-ai-lab/harth-ml-experiments>

DeepConvLSTM [33] applies convolutional layers to automatically learn feature representations and LSTM to model the temporal dependencies between their activations.

XGBoost [8] is a scalable end-to-end machine learning system for tree boosting, which has been widely recognized in machine learning and time-series analysis.

MA-CNN [37] first extracts preliminary features for each sensing modality through its own dedicated convolutional layers, then the extracted intra-sensor features are combined through fully-connected layers for human activity recognition.

HHAR-net [14] builds a two-level hierarchical classification model by first dividing the activities into “stationary” and “non-stationary”. The Opportunity dataset only has non-stationary activities, in this case the method degrades to a one-level classification.

Rocket [12] applies a large number of random convolution kernels (kernels with random weights, bias, etc.) to transform the time-series data, each of which approximately captures a relevant feature. Then a classifier is trained based on the transformed features.

THAT [25] proposes a two-stream convolution augmented human activity transformer which captures both time-over-channel and channel-over-time features in a two-stream structure.

TST [54] is a Transformer-based representation learning framework with downstream tasks of multivariate time-series classification and regression. We follow the framework to first pre-train the Transformer model in an unsupervised fashion, and then fine-tune the pre-trained model on the downstream classification task.

We evaluate the performance of SemanticHAR and baselines using accuracy and macro-F1 as metrics. Macro-F1 is defined as $\text{macro-F1} = \frac{1}{N} \sum_{i=1}^N 2 \times \frac{\text{Prec}_i \times \text{Rec}_i}{\text{Prec}_i + \text{Rec}_i}$, where $\text{Prec}_i, \text{Rec}_i$ represent the precision and recall for each category i , and N is the total number of activity categories.

6.1 Experimental Setup

We use a two-layer convolutional neural network as the encoder for extracting features. The kernel sizes for both layers are set to 3 and each layer is followed by batch normalization. We adopt LSTM with hidden dimension of 128 as the decoder, based on a grid search of {64, 128, 256}. We randomly initialize the linear embedding layer. We also tried pre-trained Glove embeddings as initialization but the performance was similar. We use Adam optimizer with learning rate $1e^{-4}$ based on a grid search of $\{1e^{-5}, 1e^{-4}, 1e^{-3}, 1e^{-2}\}$ and batch size 16. For all datasets, we further randomly split the training set into 80% for training and 20% for validation. We conduct the experiments in PyTorch with NVIDIA RTX A6000 (with 48GB memory), AMD EPYC 7452 32-Core Processor and Ubuntu 18.04.5 LTS. We tune the hyper-parameters of both SemanticHAR and baselines on the validation set, and then combine training and validation set to re-train the models after hyper-parameter tuning.

6.2 Results

We repeat 5 runs and report on the average accuracy, macro-F1 score and standard deviations of SemanticHAR and baselines in Table 2. As shown in the results, SemanticHAR consistently outperforms both statistical and deep learning-based human activity recognition and time-series classification approaches, under both metrics (accuracy and macro-F1 score). SemanticHAR reduces the

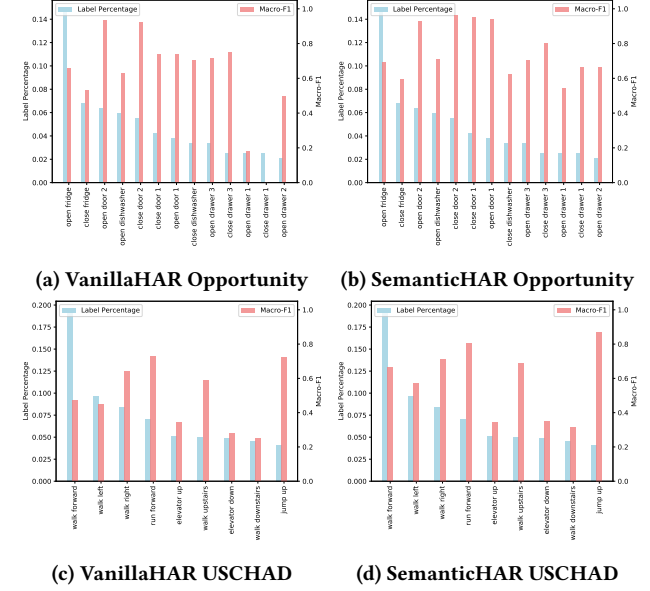


Figure 5: Macro-F1 of each activity for SemanticHAR and VanillaHAR on datasets with long-tail label distribution.

error rate by approximately 19%, 23%, 31%, 6%, 8%, 5% on the six HAR datasets, respectively. The best performing baselines are Rocket, TST and THAT, but these methods propose better feature extractors or representation learning methods in order to improve recognition performance, but do not take account of the label name semantics. SemanticHAR is capable of leveraging the inherent shared structure in label names, thus achieving the highest accuracy and macro-F1 score. We notice that the performance improvement is especially significant for the Opportunity dataset, as this dataset has the largest number of shared label names.

6.3 Ablations

To verify the effectiveness of our sequence-to-sequence architecture SemanticHAR through decoding label names, we also compare SemanticHAR with some ablations listed as follows. For all the ablations, we use the same encoder for feature extraction as SemanticHAR.

VanillaHAR: We use the same encoder as SemanticHAR to extract features embedded in the data, and directly append a linear layer for classification without label name modeling.

label modeling using Glove embeddings: We also design a variant which has two separate linear branches at end. One branch is for classifying the labels, and the other branch predicts embeddings for the label names. During training, apart from the classification loss, we maximize the cosine similarity between the predicted embeddings and the pre-trained Glove embeddings [34]. If the label names have multiple words, we use the average Glove embedding of each word as the embedding for the entire label name.

label modeling using fasttext embeddings: same as previous one, replace Glove embeddings with fasttext embeddings [5].

multi-label classification: We also tried treating both activity sequences (e.g., “eating soup”) as well as shared tokens (e.g., “eating”)

Table 3: Accuracy and Macro-F1 on Mhealth dataset. We bold the best score and underline the second best.

Datasets	Metrics	DeepConvLSTM	XGBoost	MA-CNN	HHAR-net	THAT	Rocket	TST	SemanticHAR
Mhealth	Accuracy	0.868±0.023	0.809±0.011	0.839±0.010	0.854±0.020	<u>0.907±0.019</u>	0.902±0.006	0.863±0.007	0.949±0.017
	Macro-F1	0.871±0.023	0.775±0.023	0.834±0.009	0.811±0.022	<u>0.910±0.017</u>	0.908±0.007	0.863±0.007	0.949±0.019

Table 4: Original and modified label names for Mhealth dataset.

Original Label Names	Modified Label Names
standing still	leg still
sitting and relaxing	buttocks still
lying down	back down
walking	leg walk
climbing stairs	leg up
waist bends forward	back forward
frontals elevation of arms	arm up
knees bending (crouching)	leg forward
cycling	leg cycle
jogging	leg jog
running	leg jog fast
jump front and back	leg jump

Table 5: Accuracy and Macro-F1 score compared with using non-overlapping label names.

Method	VanillaHAR	Non-best baseline		SemanticHAR
		Overlapping	best	
Accuracy	0.7574	0.7617	0.8110	0.8468
Macro-F1	0.6178	0.6739	0.6912	0.7414

as classes. The classes of shared tokens help learn dependencies across activities, and during testing we only compare scores from classes of the original activity sequences.

no label aug: We stay with the sequence-to-sequence architecture but remove label augmentation during training.

We report performance of different ablations in Table 6, and also list the best baseline performance from Table 2 for reference. We notice that there exist significant improvements from only applying feature encoder to the proposed sequence-to-sequence architecture that decodes label names. Regressing label name embeddings by optimizing a cosine similarity loss compared with Glove or fast-text embeddings slightly improves the performance. This demonstrates that only incorporating word embeddings does not explicitly take into account the shared label name structure and stays sub-optimal, while generating label names decomposes learning activities into separate tokens and encourages knowledge sharing for more efficient learning. Compared with multi-label classification, our sequence-to-sequence approach better preserves the word order (n-gram) and word correlation information in the label sequence. For example, multi-label approach cannot well distinguish activities whose label names are part of other activity names (e.g., “walk” and “walk upstairs”). Moreover, the performance degrades after removing label augmentation, which validates its importance in capturing shared word semantics during training.

6.4 Generating Shared Label Names

Some HAR datasets may not have shared tokens in their original names. In this case, we use OpenAI’s recently released ChatGPT to automatically generate label names with shared tokens. We send the following prompt to ChatGPT: *Describe the following activities one by one with information of 1. body part used, 2. action, 3. object, 4. adverb.* As human activities naturally have shared actions and objects, the prompt helps find common tokens across activities. With the aid of ChatGPT, such process is performed with minimal human expert efforts. Based on the structured information provided by ChatGPT, we can summarize the label names with shared tokens. We apply the above process on Mhealth dataset [4] (publicly available at UCI Machine Learning Repository⁷) and summarize the original and modified label names in Table 4. We also compare SemanticHAR with modified label names against the baselines on Mhealth dataset in Table 3, and observed state-of-the-art performance.

6.5 Few-Shot Settings

We further examine the model performance under few-shot settings. We randomly reduce the number of samples in the training set from two HAR datasets to 20%, 40%, 60%, 80%, and evaluate the macro-F1 on the same original test set. Figure 6a illustrates the performance trend of SemanticHAR, VanillaHAR as well as the best performing baselines. As we could observe from the figure, the macro-F1 generally increases as the number of available training data increases. On top of that, the performance gap between SemanticHAR and other methods in general remains larger when there are fewer available training data, as decoding label name helps learn the common semantic sub-structure that is shared across different classes.

The above experiment reduces training samples for all the classes. Many HAR datasets also naturally have a long-tail distribution where some activities have fewer samples as being more difficult in terms of data collection. We also evaluate such label imbalance scenario as shown in Figure 5. We compare SemanticHAR and the vanilla classification model VanillaHAR by visualizing the example activities with shared tokens. The activity names are sorted in a decreasing order of the label percentage in the dataset (blue or left bars in the figure). The performance grows significantly (red or right bars in the figure) when adopting the sequence-to-sequence architecture, as decoding label names helps transfer the shared word semantics to those classes with fewer available samples. For example, for the tail classes “open drawer 1”, “close drawer 1”, “open drawer 2”, VanillaHAR shows low F1 score (even zero for “close drawer 1”), while SemanticHAR substantially improves the performance on these classes, as SemanticHAR is able to leverage label semantics structure to learn from other classes.

⁷<http://archive.ics.uci.edu/ml/datasets/mhealth+dataset>

Table 6: Accuracy and Macro-F1 for different model ablations. We bold the best score and underline the second best.

Datasets	Metrics	VanillaHAR no label modeling	label modeling using Glove	label modeling using fasttext	multi label	no label aug	best baseline	SemanticHAR
Opp	Accuracy	0.737±0.022	0.753±0.008	0.758±0.013	0.761±0.011	0.819±0.005	0.811±0.008	0.847±0.015
	Macro-F1	0.604±0.023	0.619±0.015	0.633±0.020	0.619±0.009	0.732±0.014	0.691±0.015	<u>0.741±0.029</u>
PAMAP2	Accuracy	0.921±0.033	0.928±0.022	0.930±0.018	0.881±0.008	0.951±0.006	0.943±0.005	0.956±0.007
	Macro-F1	0.924±0.024	0.934±0.022	0.935±0.017	0.891±0.010	0.960±0.006	0.949±0.005	<u>0.964±0.007</u>
UCI-HAR	Accuracy	0.921±0.005	0.922±0.007	0.924±0.002	0.681±0.018	0.954±0.006	0.939±0.002	0.958±0.003
	Macro-F1	0.921±0.005	0.922±0.008	0.924±0.002	0.620±0.030	0.953±0.006	0.942±0.002	<u>0.958±0.003</u>
USCHAD	Accuracy	0.543±0.028	0.545±0.027	0.552±0.029	0.548±0.013	0.622±0.050	0.643±0.015	0.663±0.011
	Macro-F1	0.538±0.024	0.538±0.027	0.546±0.022	0.551±0.014	0.600±0.029	0.619±0.012	<u>0.623±0.009</u>
WISDM	Accuracy	0.644±0.006	0.642±0.013	0.647±0.008	0.662±0.004	0.786±0.008	0.774±0.005	0.793±0.007
	Macro-F1	0.639±0.006	0.636±0.013	0.641±0.010	0.655±0.004	0.783±0.008	0.767±0.004	<u>0.786±0.008</u>
Harth	Accuracy	0.977±0.005	0.981±0.003	0.976±0.004	0.976±0.005	0.981±0.006	<u>0.981±0.001</u>	0.982±0.003
	Macro-F1	0.481±0.004	0.484±0.004	0.481±0.003	0.480±0.004	0.566±0.034	0.578±0.032	<u>0.583±0.020</u>

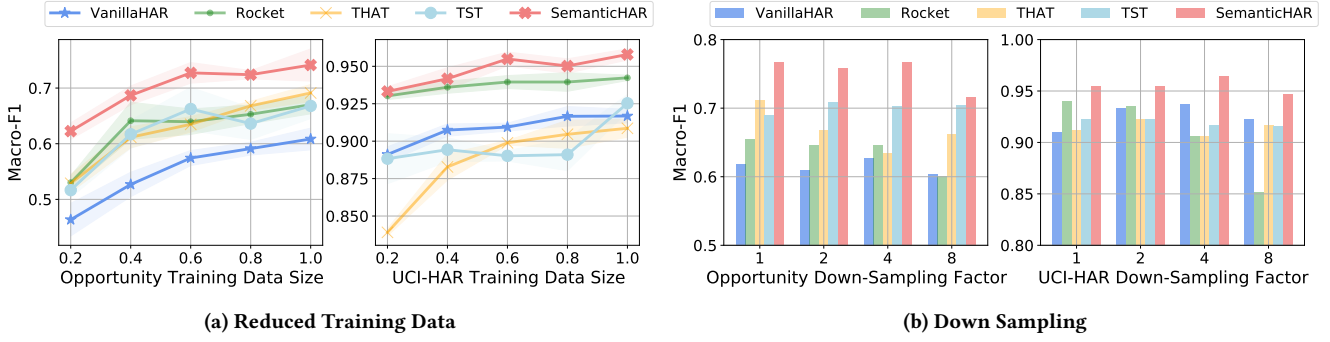


Figure 6: Macro-F1 of SemanticHAR, VanillaHAR and best performing baselines with reduced and down-sampled data.

6.6 HAR with Non-Overlapping Words as Labels

To evaluate the capability of SemanticHAR on learning shared label names, we manually replace the original label names to non-overlapping single numbers. Specifically, each label $y_i = i$ becomes a single number after replacement. We evaluate SemanticHAR using this new label set and report as “non-overlapping” in Table 5. We also list the performance of VanillaHAR and best baseline from Table 2 and Table 6 for reference. As we can observe from the table, there exists performance improvement from VanillaHAR to SemanticHAR under non-overlapping label set. The potential reasons include change of loss function, change of model parameter size, etc. However, the largest improvement lies between SemanticHAR under non-overlapping label set and SemanticHAR under original shared label names (last column in Table 5). This indicates that majority of the performance gains of SemanticHAR originate from leveraging shared label names across activities.

6.7 Sensitivity Analysis

We also perform a sensitivity analysis with respect to the sampling frequency of different HAR datasets. We down sample both training and test set by a factor of 2,4,8 and report on the performance of SemanticHAR, VanillaHAR as well as the best performing baselines in Figure 6b. VanillaHAR, Rocket and THAT are more sensitive to down-sampling factors, as sampling frequency affects the

granularity of local features, and different methods differ in the optimal granularity. TST leverages the benefits from representation learning and appears to be more robust with respect to different sampling frequencies. SemanticHAR also stays robust with respect to down-sampling factors, as it encourages more efficient learning via modeling label name semantics. We observe that our proposed SemanticHAR consistently outperforms VanillaHAR and baselines under different down-sampling factors.

7 CONCLUSIONS

We observe that semantically similar label names also indicate resemblance in the input sensory data. Instead of formulating the task as a classification problem as existing HAR methods do, we cast the task as a sequence-to-sequence decoding problem, where correct prediction translates to decoding ground truth label names with the highest probability. This approach ensures that similar activities have close structured output, thus transferring learnt knowledge across different activities and alleviating the challenges of annotated data shortage in HAR. We evaluated SemanticHAR on seven HAR datasets, and results demonstrate that our model outperforms state-of-the-art baselines.

Going forward, we plan to design more complex backbone models and adapt the proposed model to other data modalities like images and videos, as many human activity recognition tasks are also based on image or video data, as well as other types of datasets

that also have shared label name structure, e.g., medical datasets with shared disease names. We also plan to explore transfer learning across different datasets with activity names consisting of the same words.

REFERENCES

- [1] Davide Anguita, Alessandro Ghio, Luca Oneto, Xavier Parra, Jorge Luis Reyes-Ortiz, et al. 2013. A public domain dataset for human activity recognition using smartphones.. In *Eusann*, Vol. 3. 3.
- [2] Marc Bachlin, Meir Plotnik, Daniel Roggen, Inbal Maidan, Jeffrey M Hausdorff, Nir Giladi, and Gerhard Troster. 2009. Wearable assistant for Parkinson’s disease patients with the freezing of gait symptom. *IEEE Transactions on Information Technology in Biomedicine* 14, 2 (2009), 436–446.
- [3] Anthony Bagnall, Hoang Anh Dau, Jason Lines, Michael Flynn, James Large, Aaron Bostrom, Paul Southam, and Eamonn Keogh. 2018. The UEA multivariate time series classification archive, 2018. *arXiv preprint arXiv:1811.00075* (2018).
- [4] Oresti Banos, Rafael Garcia, Juan A Holgado-Terriza, Miguel Damas, Hector Pomares, Ignacio Rojas, Alejandro Saez, and Claudia Villalonga. 2014. mHealth-Droid: a novel framework for agile development of mobile health applications. In *International workshop on ambient assisted living*. Springer, 91–98.
- [5] Piotr Bojanowski, Edouard Grave, Armand Joulin, and Tomas Mikolov. 2017. Enriching word vectors with subword information. *Transactions of the Association for Computational Linguistics* 5 (2017), 135–146.
- [6] Kaixuan Chen, Lina Yao, Dalin Zhang, Xiaojun Chang, Guodong Long, and Sen Wang. 2019. Distributionally robust semi-supervised learning for people-centric sensing. In *Proceedings of the AAAI Conference on Artificial Intelligence*, Vol. 33.
- [7] Kaixuan Chen, Dalin Zhang, Lina Yao, Bin Guo, Zhiwen Yu, and Yunhao Liu. 2021. Deep learning for sensor-based human activity recognition: Overview, challenges, and opportunities. *ACM Computing Surveys (CSUR)* 54, 4 (2021).
- [8] Tianqi Chen and Carlos Guestrin. 2016. Xgboost: A scalable tree boosting system. In *Proceedings of the 22nd ACM SIGKDD international conference on knowledge discovery and data mining*, 785–794.
- [9] Belkacem Chikhaoui and Frank Gouineau. 2017. Towards automatic feature extraction for activity recognition from wearable sensors: a deep learning approach. In *2017 IEEE International Conference on Data Mining Workshops (ICDMW)*. IEEE.
- [10] Ranak Roy Chowdhury, Xiyuan Zhang, Jingbo Shang, Rajesh K Gupta, and Dezhong Hong. 2022. TARNNet: Task-Aware Reconstruction for Time-Series Transformer. In *Proceedings of the 28th ACM SIGKDD Conference on Knowledge Discovery and Data Mining*, Washington, DC, USA, 14–18.
- [11] Zhicheng Cui, Wenlin Chen, and Yixin Chen. 2016. Multi-scale convolutional neural networks for time series classification. *arXiv preprint arXiv:1603.06995* (2016).
- [12] Angus Dempster, François Petitjean, and Geoffrey I Webb. 2020. ROCKET: exceptionally fast and accurate time series classification using random convolutional kernels. *Data Mining and Knowledge Discovery* 34, 5 (2020), 1454–1495.
- [13] Angus Dempster, Daniel F Schmidt, and Geoffrey I Webb. 2021. Minirocket: A very fast (almost) deterministic transform for time series classification. In *Proceedings of the 27th ACM SIGKDD Conference on Knowledge Discovery & Data Mining*, 248–257.
- [14] Mehrdad Fazli, Kamran Kowsari, Erfan Gharavi, Laura Barnes, and Afsaneh Doryab. 2021. HHAR-net: hierarchical human activity recognition using neural networks. In *International Conference on Intelligent Human Computer Interaction*. Springer, 48–58.
- [15] Davide Figo, Pedro C Diniz, Diogo R Ferreira, and Joao MP Cardoso. 2010. Pre-processing techniques for context recognition from accelerometer data. *Personal and Ubiquitous Computing* 14, 7 (2010), 645–662.
- [16] Yu Guan and Thomas Plötz. 2017. Ensembles of deep lstm learners for activity recognition using wearables. *Proceedings of the ACM on Interactive, Mobile, Wearable and Ubiquitous Technologies* 1, 2 (2017), 1–28.
- [17] Nils Y Hammerla, Shane Halloran, and Thomas Plötz. 2016. Deep, convolutional, and recurrent models for human activity recognition using wearables. *arXiv preprint arXiv:1604.08860* (2016).
- [18] Sepp Hochreiter and Jürgen Schmidhuber. 1997. Long short-term memory. *Neural computation* 9, 8 (1997), 1735–1780.
- [19] HM Sajjad Hossain and Nirmalya Roy. 2019. Active deep learning for activity recognition with context aware annotator selection. In *KDD*, 1862–1870.
- [20] Hassan Ismail Fawaz, Benjamin Lucas, Germain Forestier, Charlotte Pelletier, Daniel F Schmidt, Jonathan Weber, Geoffrey I Webb, Lhassane Idoumghar, Pierre-Alain Muller, and François Petitjean. 2020. Inceptiontime: Finding alexnet for time series classification. *Data Mining and Knowledge Discovery* 34, 6 (2020), 1936–1962.
- [21] Jeya Vikranth Jeyakumar, Liangzhen Lai, Naveen Suda, and Mani Srivastava. 2019. SenseHAR: a robust virtual activity sensor for smartphones and wearables. In *Proceedings of the 17th Conference on Embedded Networked Sensor Systems*.
- [22] Fazle Karim, Somshubra Majumdar, Houshang Darabi, and Shun Chen. 2017. LSTM fully convolutional networks for time series classification. *IEEE access* 6 (2017), 1662–1669.
- [23] Fazle Karim, Somshubra Majumdar, Houshang Darabi, and Samuel Harford. 2019. Multivariate LSTM-FCNs for time series classification. *Neural Networks* 116 (2019), 237–245.
- [24] Jimmy Lei Ba, Kevin Swersky, Sanja Fidler, et al. 2015. Predicting deep zero-shot convolutional neural networks using textual descriptions. In *Proceedings of the IEEE international conference on computer vision*, 4247–4255.
- [25] Bing Li, Wei Cui, Wei Wang, Le Zhang, Zhenghua Chen, and Min Wu. 2021. Two-stream convolution augmented transformer for human activity recognition. In *Proceedings of the AAAI Conference on Artificial Intelligence*, Vol. 35. 286–293.
- [26] Chenglin Li, Di Niu, Bei Jiang, Xiao Zuo, and Jianming Yang. 2021. Meta-har: Federated representation learning for human activity recognition. In *Proceedings of the Web Conference 2021*. 912–922.
- [27] Guozhong Li, Byron Choi, Jianliang Xu, Sourav S Bhowmick, Kwok-Pan Chun, and Grace LH Wong. 2021. Shapenet: A shapelet-neural network approach for multivariate time series classification. In *Proceedings of the AAAI Conference on Artificial Intelligence*, Vol. 35. 8375–8383.
- [28] Jason Lines, Sarah Taylor, and Anthony Bagnall. 2018. Time series classification with HIVE-COTE: The hierarchical vote collective of transformation-based ensembles. *ACM Transactions on Knowledge Discovery from Data* 12, 5 (2018).
- [29] Aleksej Logacjov, Kerstin Bach, Atle Kongsvold, Hilde Bremseth Bärdstu, and Paul Jarle Mork. 2021. HARTH: A Human Activity Recognition Dataset for Machine Learning. *Sensors* 21, 23 (2021), 7853.
- [30] Haojie Ma, Wenzhong Li, Xiao Zhang, Songcheng Gao, and Sanglu Lu. 2019. AttnSense: Multi-level Attention Mechanism For Multimodal Human Activity Recognition.. In *IJCAI*. 3109–3115.
- [31] Yuchao Ma and Hassan Ghasemzadeh. 2019. LabelForest: Non-parametric semi-supervised learning for activity recognition. In *Proceedings of the AAAI Conference on Artificial Intelligence*, Vol. 33. 4520–4527.
- [32] Moe Matsuki, Paula Lago, and Sozo Inoue. 2019. Characterizing word embeddings for zero-shot sensor-based human activity recognition. *Sensors* 19, 22 (2019), 5043.
- [33] Francisco Javier Ordóñez and Daniel Roggen. 2016. Deep convolutional and lstm recurrent neural networks for multimodal wearable activity recognition. *Sensors* 16, 1 (2016), 115.
- [34] Jeffrey Pennington, Richard Socher, and Christopher D Manning. 2014. Glove: Global vectors for word representation. In *Proceedings of the 2014 conference on empirical methods in natural language processing (EMNLP)*. 1532–1543.
- [35] Hangwei Qian, Sinno Pan, and Chunyan Miao. 2018. Sensor-based activity recognition via learning from distributions. In *Proceedings of the AAAI Conference on Artificial Intelligence*, Vol. 32.
- [36] Alex Radford, Joon Wool Kim, Chris Hallacy, Aditya Ramesh, Gabriel Goh, Sandhini Agarwal, Girish Sastry, Amanda Askell, Pamela Mishkin, Jack Clark, et al. 2021. Learning transferable visual models from natural language supervision. In *International Conference on Machine Learning*. PMLR, 8748–8763.
- [37] Valentin Radu, Catherine Tong, Sourav Bhattacharya, Nicholas D Lane, Cecilia Mascolo, Mahesh K Marina, and Fahim Kawsar. 2018. Multimodal deep learning for activity and context recognition. *Proceedings of the ACM on Interactive, Mobile, Wearable and Ubiquitous Technologies* 1, 4 (2018), 1–27.
- [38] Attila Reiss and Didier Stricker. 2012. Introducing a new benchmarked dataset for activity monitoring. In *2012 16th international symposium on wearable computers*. IEEE, 108–109.
- [39] Daniel Roggen, Alberto Calatroni, Mirco Rossi, Thomas Holleczek, Kilian Förster, Gerhard Tröster, Paul Lukowicz, David Bannach, Gerald Pirk, Alois Ferscha, et al. 2010. Collecting complex activity datasets in highly rich networked sensor environments. In *2010 Seventh international conference on networked sensing systems (INSS)*. IEEE, 233–240.
- [40] Patrick Schäfer and Ulf Leser. 2017. Multivariate time series classification with WEASEL+ MUSE. *arXiv preprint arXiv:1711.11343* (2017).
- [41] Ahmed Shifaz, Charlotte Pelletier, François Petitjean, and Geoffrey I Webb. 2020. TS-CHIEF: a scalable and accurate forest algorithm for time series classification. *Data Mining and Knowledge Discovery* 34, 3 (2020), 742–775.
- [42] Mohammad Shokoh-Yekta, Jun Wang, and Eamonn Keogh. 2015. On the non-trivial generalization of dynamic time warping to the multi-dimensional case. In *Proceedings of the 2015 SIAM international conference on data mining*. SIAM, 289–297.
- [43] Wensi Tang, Guodong Long, Lu Liu, Tianyi Zhou, Michael Blumenstein, and Jing Jiang. 2021. Omni-Scale CNNs: a simple and effective kernel size configuration for time series classification. In *International Conference on Learning Representations*.
- [44] Catherine Tong, Jinchen Ge, and Nicholas D Lane. 2021. Zero-Shot Learning for IMU-Based Activity Recognition Using Video Embeddings. *Proceedings of the ACM on Interactive, Mobile, Wearable and Ubiquitous Technologies* 5, 4 (2021), 1–23.
- [45] Laura Von Rueden, Sebastian Mayer, Katharina Beckh, Bogdan Georgiev, Sven Giesselbach, Raoul Heese, Birgit Kirsch, Julius Pfrommer, Annika Pick, Rajkumar Ramamurthy, et al. 2019. Informed Machine Learning—A Taxonomy and Survey

of Integrating Knowledge into Learning Systems. *arXiv preprint arXiv:1903.12394* (2019).

[46] Zhiguang Wang, Weizhong Yan, and Tim Oates. 2017. Time series classification from scratch with deep neural networks: A strong baseline. In *2017 International joint conference on neural networks (IJCNN)*. IEEE, 1578–1585.

[47] Gary M Weiss, Kenichi Yoneda, and Thaier Hayajneh. 2019. Smartphone and smartwatch-based biometrics using activities of daily living. *IEEE Access* 7 (2019), 133190–133202.

[48] Waskitho Wibisono, Dedy Nur Arifin, Baskoro Adi Pratomo, Tohari Ahmad, and Royyana M Ijtihadie. 2013. Falls detection and notification system using tri-axial accelerometer and gyroscope sensors of a smartphone. In *2013 Conference on Technologies and Applications of Artificial Intelligence*. IEEE, 382–385.

[49] Ronald J Williams and David Zipser. 1989. A learning algorithm for continually running fully recurrent neural networks. *Neural computation* 1, 2 (1989), 270–280.

[50] Tong Wu, Yiqiang Chen, Yang Gu, Jiwei Wang, Siyu Zhang, and Zhanghu Zhechen. 2020. Multi-layer cross loss model for zero-shot human activity recognition. In *Pacific-Asia Conference on Knowledge Discovery and Data Mining*. Springer, 210–221.

[51] Qiao Xiao, Boqian Wu, Yu Zhang, Shiwei Liu, Mykola Pechenizkiy, Elena Mocanu, and Decebal Constantin Mocanu. 2022. Dynamic Sparse Network for Time Series Classification: Learning What to “see”. *arXiv preprint arXiv:2212.09840* (2022).

[52] Jianbo Yang, Minh Nhut Nguyen, Phyto Phyto San, Xiao Li Li, and Shonali Krishnaswamy. 2015. Deep convolutional neural networks on multichannel time series for human activity recognition. In *Twenty-fourth international joint conference on artificial intelligence*.

[53] Shuochao Yao, Shaohan Hu, Yiran Zhao, Aston Zhang, and Tarek Abdelzaher. 2017. Deepsense: A unified deep learning framework for time-series mobile sensing data processing. In *Proceedings of the 26th International Conference on World Wide Web*, 351–360.

[54] George Zerveas, Srideepika Jayaraman, Dhaval Patel, Anuradha Bhamidipaty, and Carsten Eickhoff. 2021. A transformer-based framework for multivariate time series representation learning. In *Proceedings of the 27th ACM SIGKDD Conference on Knowledge Discovery & Data Mining*, 2114–2124.

[55] Daochen Zha, Kwei-Herng Lai, Kaixiong Zhou, and Xia Hu. 2022. Towards Similarity-Aware Time-Series Classification. *arXiv preprint arXiv:2201.01413* (2022).

[56] Mi Zhang and Alexander A Sawchuk. 2012. USC-HAD: A daily activity dataset for ubiquitous activity recognition using wearable sensors. In *Proceedings of the 2012 ACM conference on ubiquitous computing*, 1036–1043.

[57] Shibo Zhang, Yaxuan Li, Shen Zhang, Farzad Shahabi, Stephen Xia, Yu Deng, and Nabil Alshurafa. 2021. Deep Learning in Human Activity Recognition with Wearable Sensors: A Review on Advances. *arXiv preprint arXiv:2111.00418* (2021).

[58] Xuchao Zhang, Yifeng Gao, Jessica Lin, and Chang-Tien Lu. 2020. Tapnet: Multivariate time series classification with attentional prototypical network. In *Proceedings of the AAAI Conference on Artificial Intelligence*, Vol. 34, 6845–6852.

[59] Fengtao Zhou, Sheng Huang, and Yun Xing. 2021. Deep semantic dictionary learning for multi-label image classification. In *Proceedings of the AAAI Conference on Artificial Intelligence*, Vol. 35, 3572–3580.